

Arsenic behavior across soil-water interfaces in paddy soils: coupling, decoupling and speciation

YUAN, Zhao-Feng, GUSTAVE, Williamson, BOYLE, John, SEKAR, Raju <<http://orcid.org/0000-0002-1182-9004>>, BRIDGE, Jonathan <<http://orcid.org/0000-0003-3717-519X>>, REN, Yuxiang, TANG, Xianjin, GUO, Bin and CHEN, Zheng

Available from Sheffield Hallam University Research Archive (SHURA) at:

<http://shura.shu.ac.uk/27526/>

This document is the author deposited version. You are advised to consult the publisher's version if you wish to cite from it.

Published version

YUAN, Zhao-Feng, GUSTAVE, Williamson, BOYLE, John, SEKAR, Raju, BRIDGE, Jonathan, REN, Yuxiang, TANG, Xianjin, GUO, Bin and CHEN, Zheng (2020). Arsenic behavior across soil-water interfaces in paddy soils: coupling, decoupling and speciation. *Chemosphere*, p. 128713.

Copyright and re-use policy

See <http://shura.shu.ac.uk/information.html>

1 **Title: Arsenic behavior across soil-water interfaces in paddy soils:**
2 **coupling, decoupling and speciation**

3 **Names of authors:** Zhao-Feng Yuan ^{1, 2}, Williamson Gustave ^{1, 2, 3}, John Boyle ⁴, Raju Sekar ⁵,
4 Jonathan Bridge ⁶, Yuxiang Ren ¹, Xianjin Tang ⁷, Bin Guo ^{8*} and Zheng Chen ^{1*}

5 ¹ Department of Health and Environmental Sciences, Xi'an Jiaotong-Liverpool University, 111 Ren'ai
6 Road, Suzhou, Jiangsu 215123, China.

7 ² Department of Environmental Science, University of Liverpool, Brownlow Hill, Liverpool L69 7ZX,
8 UK.

9 ³ Chemistry, Environmental & Life Sciences, University of The Bahamas, New Providence, Nassau,
10 The Bahamas.

11 ⁴ Department of Geography & Planning, University of Liverpool, Roxby Building, Liverpool, L69 7ZT,
12 UK.

13 ⁵ Department of Biological Sciences, Xi'an Jiaotong-Liverpool University, 111 Ren'ai Road, Suzhou,
14 Jiangsu 215123, China.

15 ⁶ Department of Natural and Built Environment, Sheffield Hallam University, Howard St, Sheffield S1
16 1WB, UK.

17 ⁷ Institute of Soil and Water Resources and Environmental Science, Zhejiang Provincial Key
18 Laboratory of Agricultural Resources and Environment, Zhejiang University, 866 Yuhangtang Road,
19 Hangzhou 310058, China.

20 ⁸ Institute of Environment, Resource, Soil and Fertilizer, Zhejiang Academy of Agricultural Sciences,
21 Hangzhou, 310021, China.

22

23 * **Corresponding author:** Bin Guo (Email: ndgb@163.com); Zheng Chen (E-mail:
24 ebiogeochem@outlook.com or Zheng.Chen@xjtlu.edu.cn; Tel: +86-512-81880471; fax:
25 +86-512-88161899).

26 **Abstract**

27 The sharp redox gradient at soil-water interfaces (SWI) plays a key role in controlling
28 arsenic (As) translocation and transformation in paddy soils. When Eh drops, As is
29 released to porewater from solid iron (Fe) and manganese (Mn) minerals and reduced
30 to arsenite. However, the coupling or decoupling processes operating within the redox
31 gradient at the SWI in flooded paddy soils remain poorly constrained due to the lack
32 of direct evidence. In this paper, we reported the mm-scale mapping of Fe, As and
33 other associated elements across the redox gradient in the SWI of five different paddy
34 soils. The results showed a strong positive linear relationship between dissolved Fe,
35 Mn, As, and phosphorus (P) in 4 out of the 5 paddy soils, indicating the general
36 coupling of these elements. However, decoupling of Fe, Mn and As was observed in
37 one of the paddy soils. In this soil, distinct releasing profiles of Mn, As and Fe were
38 observed, and the releasing order followed the redox ladder. Further investigation of
39 As species showed the ratio of arsenite to total As dropped from 100% to 75.5% and
40 then kept stable along depth of the soil profile, which indicates a dynamic equilibrium
41 between arsenite oxidization and arsenate reduction. This study provides direct
42 evidence of multi-elements' interaction along redox gradient of SWI in paddy soils.

43

44 **Keywords:** arsenic, iron, profile, paddy soil, coupling, decoupling

45

46 **1. Introduction**

47 Paddy fields globally represent artificial wetlands, supporting the growth of rice
48 (Bouman and Tuong, 2001). Paddy agriculture for the production of rice involves
49 intermittent flooding to favor the growth of rice and in some cases to reduce the
50 bioavailability of cadmium (Hu et al., 2015). During the flooding stage,
51 redox-sensitive elements in the soil, such as iron (Fe) and manganese (Mn), may
52 become mobile from the solid into the liquid phase (Xu et al., 2017; Zhang et al.,
53 2018), and lead to dissolution of the sorbates (e.g. arsenic (As), and phosphorus (P))
54 bound on the solid phase (act as sorbents) (Darland and Inskeep, 1997; Polizzotto et
55 al., 2008). Other redox-sensitive elements, such as sulfur (S), may become immobile
56 from the liquid to solid phase, and result in immobilization of dissolved elements
57 through co-precipitation (e.g. FeS, As₂S₃) or adsorption (Burton et al., 2008). Among
58 the noted elements, the mobilization of As is of particular concern since rice plants
59 can efficiently uptake and accumulate As in their rice grains (Honma et al., 2016;
60 Gustave et al., 2019a). This poses a threat to human health since long-term As
61 exposure is known to cause cancer and organ failure (Meharg, 2004; Roberts et al.,
62 2010). Understanding the biogeochemical cycling of As in paddy soils under
63 heterogeneous and transient geochemical conditions during flooding and drainage is
64 therefore of high importance in predicting and thus mitigating its uptake into food
65 crops.

66 Arsenic behavior in saturated soils is closely coupled to that of Fe oxides. This
67 occurs because Fe oxides provide the main adsorption sites for As (Zobrist et al., 2000;
68 Chen et al., 2006; Tufano et al., 2008). When paddy soils are flooded, Fe oxides are
69 reduced and dissolved by dissimilatory Fe reducing bacteria, leading to the
70 simultaneous release of adsorbed As into porewater (Takahashi et al., 2004). The term
71 “coupling of Fe and As” was used to describe this phenomenon, in which the release
72 of Fe and As into the soil porewater shows a close positive correlation (Weber et al.,
73 2010). In contrast, the term “decoupling of Fe and As” was defined to refer to the lack
74 of a linear correlation between dissolved Fe and As concentrations (Weber et al.,
75 2010).

76 Coupling of Fe and As has been well documented in soils, yet the decoupling
77 process remains not well resolved (Weber et al., 2010; Bennett et al., 2012). To clarify
78 the mechanisms regulating the potential decoupling of As and Fe, simplified water-Fe
79 minerals-bacteria systems were employed (Tufano et al., 2008; Tufano and Scott,
80 2008; Weber et al., 2010), which indicated that coupling-decoupling is
81 thermodynamically controlled. For example, Zobrist et al. identified *sulfurospirillum*
82 *barnesii* was able to reduce adsorbed arsenate [As(V)] to arsenite [As(III)] without
83 requiring dissolution of the host Fe oxides (Zobrist et al., 2000), which could be
84 caused by an energy trade-off between reduction of adsorbed As(V) and host Fe
85 minerals by microorganisms (Campbell et al., 2006) (Islam et al., 2004). However, to
86 date this has not been confirmed in soils.

87 In saturated soils, it has been a challenge to distinguish the potential decoupling
88 between Fe and As. Homogeneous saturated soils were frequently used to investigate
89 the time-dependent behaviors of Fe and As (Masscheleyn et al., 1991; White et al.,
90 2007; Weber et al., 2010; Das et al., 2016; Honma et al., 2016; Xu et al., 2017), yet
91 the potential decoupling of As and Fe was only demonstrated in few deep aquifers
92 (White et al., 2007; Das et al., 2016). In most cases, the time-series investigation is
93 unable to capture the time points and/or hotspots that decoupling of Fe and As occurs.
94 The unsuccessful identification of the decoupling process is not surprising, because
95 the Fe reduction and As releasing usually happen in sequence with little temporal
96 offset (Zhang et al., 2018). The dynamic change of Fe and As makes it hard to catch
97 the appropriate time point, even if the decoupling of Fe and As occurs.

98 When flooded, the bulk soil becomes reduced owing to the abundant organic
99 matters (Frenzel et al., 1992). At the same time, a stable redox gradient is formed
100 between the O₂-rich surface water and subsurface soil, which could significantly
101 influence the spatial distribution of redox-sensitive elements (Mucci et al., 2000;
102 Widerlund and Davison, 2007; Arsic et al., 2018). Hence, the narrow but stable soil
103 water interface (SWI) is an ideal place to study the coupling/decoupling processes of
104 Fe and As along depth (Bennett et al., 2012; Gorny et al., 2015). Although As(V)
105 reduction theoretically happened at higher redox potential (Eh) compared to Fe(III)
106 (Borch et al., 2010), few studies have detected the spatial separation of Fe(II) and As
107 species in SWI of natural soils. This could be attributed to the lack of a suitable

108 method to simultaneously measure fine-scale Fe, As and other associated elements
109 across SWI (Gorny et al., 2015).

110 We recently developed a high-throughput method to simultaneously measure
111 concentrations of multi-element (e.g. Fe, Mn, As, P and S) and their species across
112 SWI (Yuan et al., 2019; Yuan et al., 2021). The SWI profiler used in our method
113 shows a big advantage in non-destructively and repeatedly sampling of porewater at
114 high-resolution (HR) (mm level) across SWI (Yuan et al., 2019), compared with
115 traditional HR samplers (e.g. DET, peeper). The analytical technique in our method
116 makes it possible to extract all interested parameters from volume-limited (~ 100 μ L)
117 samples collected by HR samplers (Yuan et al., 2021). In this study, the method was
118 applied to reveal the coupling/decoupling process of Fe and As, as well as other
119 associated elements, including Mn, S and P. Their profiles across the SWI in five
120 paddy soils were mapped to 1) illustrate multi-element and Eh profiles in typical
121 saturated paddy soils; 2) study the coupling/decoupling behaviors among the
122 redox-sensitive elements and 3) reveal the As speciation process across the SWI.

123

124 **2. Materials and methods**

125 **2.1 Reagents, materials and solutions.** Analytical grade reagents were purchased
126 from Aladdin Chemical Reagent Co., Ltd. (Shanghai, China), unless otherwise stated.
127 Calibration standards, including As species, Fe, Mn, P, and S, were supplied by

128 Guobiao (Beijing) Testing & Certification Co., Ltd (Beijing, China). All solutions
129 were prepared with ultrapure water (18.2 MΩ cm, Millipore Corp., Bedford, USA)
130 deoxygenated by bubbling pure N₂ overnight.

131 Paddy soils with different levels of As (25.6 - 146 mg·kg⁻¹, Table S1) were collected
132 from Wenshan (WS, 23°45'N, 105°26'E), Bijie (BI, 26°39'N, 105°47'E), Wuxue (WX,
133 29°59'N, 115°38'E), Shaoguan (SG, 25°6'N, 113°38'E) and Ganzhou (GZ, 25°30'N,
134 114°36'E), China. The plow layer soil (0 - 20 cm) was sampled and directly
135 transported to the laboratory. Soils were wet mixed and sieved through a 1.0 mm
136 diameter sieve. The wet sieved soils were mixed evenly and each soil type was added
137 to three black plastic pots (inner diameter × height = 13 cm × 21 cm), with a soil
138 depth of ~15 cm (total 15 pots). Table S1 shows the selected soil properties. The soils
139 were flooded with ultrapure water and allowed to stabilize for 30 d in dark conditions,
140 with a constant room temperature (22 °C) controlled by an air-conditioner.

141 **2.2 Deployment and sampling of SWI profiler.** The SWI profiler is a recently
142 developed HR porewater sampler (Yuan et al., 2019). It has a sampling depth of 60
143 mm, with a spatial resolution of 1.7 mm. The SWI profiler was provided by Tidu
144 Environment Inc. (Suzhou, China). Fifteen SWI profilers were inserted, one per pot,
145 into the 15 pots comprising three replicates for each of WS, BI, WX, SG, and GZ
146 paddy soils, such that the uppermost 10 mm of the profile length was in overlying
147 water and the lower 50 mm buried in saturated soil. After 30 d of incubation,

148 porewater was sampled by SWI profiler. Eh profiles were simultaneously measured
149 using a custom-made platinum micro-electrode with an Ag/AgCl reference electrode.

150 Before sampling, O₂-free ultrapure water was pumped into SWI profiler as the
151 carrier solution, with an injection pump (TYD01, Lei Fu, China). After loading of the
152 carrier solution, small ions and molecules can passively diffuse from porewater into
153 SWI profiler driving by the concentration gradient. When the diffusion process
154 reached equilibrium (after 24 h), the sample was pumped out by the injection pump
155 (Fig. S1). The sample acidified with O₂-free HCl in the first sampling event was used
156 for total elements analysis (Gustave et al., 2019b). In the second sampling event (24 h
157 after the first one), the sample was preserved with O₂-free EDTA to complex metals
158 (e.g. Fe), which would facilitate As species analysis under alkali conditions
159 (Gallagher et al., 2001; Yuan et al., 2021). The collected samples were preserved at
160 4 °C fridge before downstream instrumental analysis.

161 **2.3 Total elements analysis.** Total Fe, Mn, As, P, and S obtained from SWI profiler
162 samples were measured by inductively coupled plasma-mass spectrometry (ICP-MS,
163 NexION 350X, PerkinElmer, Inc., Shelton, CT USA). The sample in 0.6 mL
164 centrifuge tube (~ 100 µL) was introduced into ICP-MS by a PFA-200 Microflow
165 Nebulizer for elemental analysis. The counts of ⁵⁷Fe⁺, ⁵⁵Mn⁺, ⁴⁷PO⁺, ⁴⁸SO⁺ and
166 ⁹¹AsO⁺ were recorded in dynamic reaction cell (DRC) or extended dynamic range
167 (EDR) mode (Yuan et al., 2021). Spiked standards were measured after every 30
168 samples as a quality control measure.

169 The ICP-MS was optimized to the following conditions: DRC (O₂, gas flow: 1.0
170 mL·min⁻¹); data only analysis; RF power: 1600W; plasma gas flow rate: 15 L·min⁻¹;
171 auxiliary gas flow: 1.2 L·min⁻¹; nebulized gas flow: 0.90 L·min⁻¹; nickel sampling and
172 skimmer cones were used. A voltage parameter in EDR mode, called “rejection
173 parameter a” (Rpa), was optimized to 0.01 for Fe, Mn and S to enable simultaneous
174 measurement of majors (e.g. Fe, Mn, S) and traces (e.g. As) by ICP-MS, following the
175 procedure described in Yuan et al. (2021).

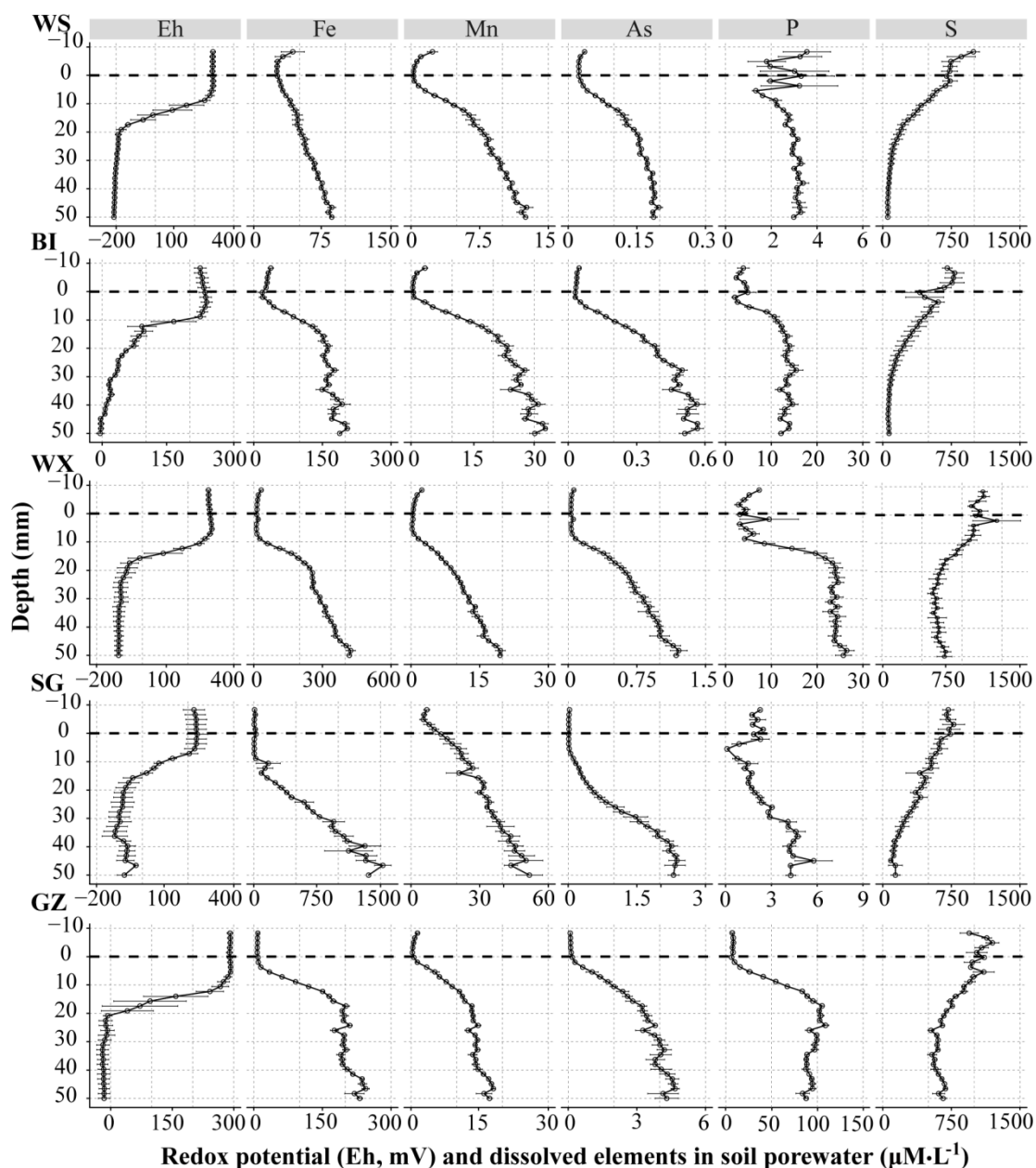
176 **2.4 Speciation of As in soil porewater.** For As speciation analysis, the ~ 100 µL
177 sample was manually loaded into a 25 µL sample loop of ion chromatography (IC,
178 Dionex ICS-1100, Thermo Scientific, USA) (Yuan et al., 2021). The IC system
179 consisted of an anion-exchange column (IonPac AS23, 250mm×4mm, Dionex).
180 Twenty mM NH₄HCO₃ (pH = 10) were used as the mobile phase (Suzuki et al., 2009;
181 Yuan et al., 2021). We expanded the comparison of As speciation in this study to
182 digitized As species published in previous reports with the Engauge Digitizing
183 software (version 11.3) used in a previous paddy soil study (Yuan et al., 2016).

184 **2.5 Statistical analysis.** Data were analyzed and plotted using R software (version
185 3.5.0). Standard errors were used to show the variance, and linear regression analysis
186 was used to identify the coupling and decoupling process of different elements.

187

188 **3. Results and discussion**

189 **3.1 Vertical changes of Eh and elements across the SWI.** The Eh (vs. Ag/AgCl
 190 reference electrode) and multi-element were measured and depicted in Fig. 1.



191

192 **Figure 1** Redox potential (Eh, mV, vs. Ag/AgCl reference electrode) and aqueous iron
 193 (Fe), manganese (Mn), arsenic (As), phosphorus (P), sulfur (S) ($\mu\text{M}\cdot\text{L}^{-1}$) across the
 194 soil-water interface. WS, BI, WX, SG and GZ represent soils collected from Wenshan,
 195 Bijie, Wuxue, Shaoguan and Ganzhou paddies respectively. The black dotted line at
 196 depth = 0 represents the soil-water interface. The error bar is standard error ($n = 3$).
 197 Note the different axis scales used.

198 The Eh changed rapidly from highly oxidizing (~ 300 mV) to reducing conditions
199 along the depth of the SWI. However, the reducing levels varied among the different
200 paddy soils. Highly reducing condition (~ -150 mV) was observed in WS/WX/SG, yet
201 a relatively moderate one (~ -10 mV) in BI/GZ. This difference in Eh might be caused
202 by different physico-chemical properties of soils. Manganese and Fe are important
203 factors for regulating soil redox (Brannon et al., 1984; Xu et al., 2017). Here, we
204 found high Mn (6.32 g·Kg⁻¹, WS) or Fe (> 70 g·Kg⁻¹, WX/SG) alone was unable to
205 buffer the decrease of soil redox (Table S1). Buffering of soil redox was only
206 achieved with both high Fe and Mn (> 70 and 1.10 g·Kg⁻¹) in BI/GZ. Although Mn is
207 believed to be the key for buffering soil redox (Xu et al., 2017), the formation of Fe
208 oxides coating with the nucleating agent is essential for nucleation and growth of Mn
209 oxides (Burns and Burns, 1975). Hence, Fe may also get involved in retarding soil
210 redox by affecting the reactivity of Mn.

211 Following Eh measurement, vertical profiles of Fe, Mn, As, P and S were
212 mapped by SWI profiler (Fig. 1). Dissolved Fe, Mn and As were almost undetectable
213 under oxidizing conditions, however their concentrations increased to $85.2 - 1359$,
214 $12.5 - 42.0$ and $0.187 - 4.31$ $\mu\text{M}\cdot\text{L}^{-1}$ respectively in reducing soils. In terms of the
215 release trend of those elements, they all showed a subsurface increase trend, which
216 agree well with previous reports of their typically vertical distributions along SWI (Di
217 et al., 2012; Wu et al., 2016a; Ma et al., 2017; Arsic et al., 2018). A similar trend was
218 also found on P. Similar to As (Xiu et al., 2016), P cycling is tightly tied to that of Fe

219 oxides in soils (Ding et al., 2016), due to Fe oxides provide the main adsorption sites
220 for P and As. The reductive mobilization of Fe, Mn, P and As was expected to
221 negatively correlate with Eh and S, nonetheless this was not always true for all the
222 paddy soils. For instance, the most As was mobilized in GZ which had a relatively
223 high Eh and S concentrations (~ -15.0 mV, $\sim 635 \mu\text{M}\cdot\text{L}^{-1}$ S, Fig. 1GZ), while the least
224 As was released in WS soil with an extremely low Eh and S (~ -200 mV, ~ 54.8
225 $\mu\text{M}\cdot\text{L}^{-1}$ S, Fig. 1WS). Similar observations to these results have been frequently
226 reported when using different soil samples (Bogdan and Schenk, 2008; Xu et al.,
227 2017). This is due to the complex process of As mobilization in soils. Although Fe
228 oxides are considered as a major agent controlling As mobilization (Xu et al., 2017), it
229 is also influenced by organic matter content, and formation of secondary minerals
230 along flooding (Bogdan and Schenk, 2008). Rich soil organic matter enhance As
231 release by accelerating biotic reduction of Fe oxides (Bogdan and Schenk, 2008). The
232 dissolved As could be re-immobilized by forming secondary minerals (like FeS, Fe₂S,
233 As₂S₃, siderite, vivianite etc.) (Bogdan and Schenk, 2008). Owing to the complex
234 biogeochemical processes involved in As mobilization, future studies should consider
235 multiple associated factors when assessing As mobilization.

236 Total dissolved S profiles have opposite trends as Fe, Mn, As and P, which
237 decreased rapidly from as high as $1000 \mu\text{M}\cdot\text{L}^{-1}$ in oxidizing conditions to a
238 concentration of $\sim 300 \mu\text{M}\cdot\text{L}^{-1}$ in reducing soil conditions. High dissolved sulfide
239 might trigger the formation of thioarsenate/thioarsenite in soil porewater (Wang et al.,

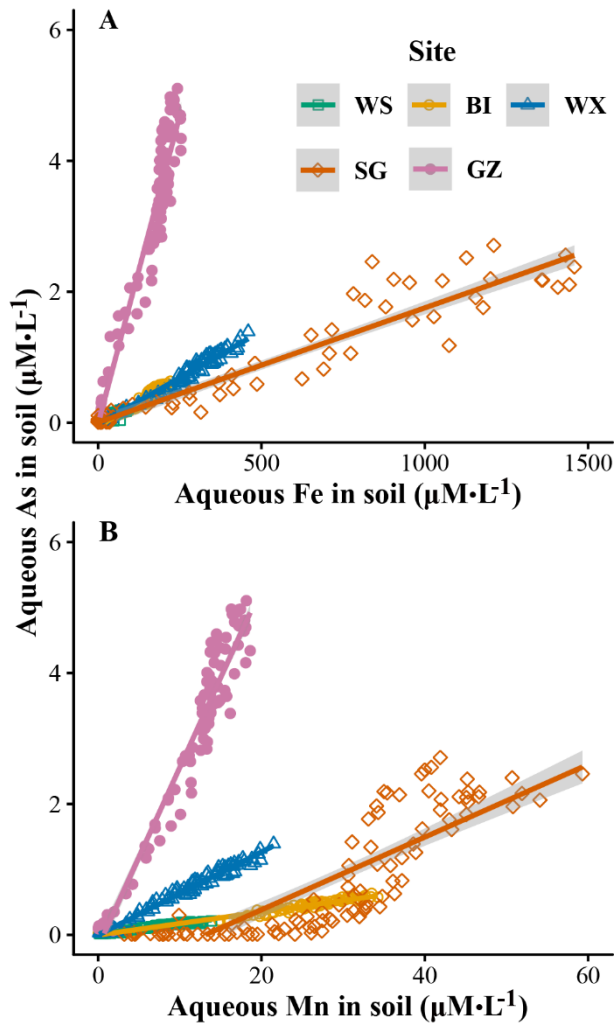
240 2020b). However, due to thioarsenate/thioarsenite was strongly suppressed by high
241 dissolved Fe in reducing soils (Wang et al., 2020b), thioarsenate/thioarsenite was not
242 detected in the oxic-anoxic transition zone in this study.

243 The decrease of S is presumably caused by sulfate reduction (Pester et al., 2012),
244 during which S(VI) is transformed to insoluble sulfide minerals by sulfate reducing
245 bacteria (Wu et al., 2016a; Wu et al., 2016b). In soils investigated, up to 85% S was
246 immobilized in WS/BI/SG, yet only 40% in WX/GZ. This difference of S fate might
247 be caused by the activity of S-reducing/oxidizing bacteria (Pester et al., 2012). Higher
248 activity of S(VI)-reducing bacteria tended to transform more soluble S(VI) to S(-II)
249 minerals (like FeS, Fe₂S etc.) (Pester et al., 2012). By contrast, higher activity of
250 S-oxidizing bacteria can sustain a larger S(VI) pool in saturated soils (Pester et al.,
251 2012).

252 **3.2 Coupling of As with Fe and Mn across SWI.** Arsenic showed a significant linear
253 relationship with Fe and Mn (Fig. 2 and Table S2). Excellent positive correlations
254 were yielded in 4 out of the 5 soils (WS, BI, WX and GZ, $R^2 \geq 0.848$, $p < 0.01$),
255 showing the tight coupling of As with Fe and Mn in typically natural soils and
256 sediments (Anawar et al., 2004; Xu et al., 2017; Arsic et al., 2018). Among the 4 soils,
257 a steeper slope of the relationship between As and Fe (~ 0.0202 , respectively) was
258 found in GZ soil than those in other soils (~ 0.00154) (Fig. 2A). The slopes may
259 depend on the content of poorly crystalline Fe oxides, which have a high affinity for
260 As (Tufano et al., 2008), and are subject to bioreduction by dissimilatory Fe reducing

261 bacteria (Zachara et al., 2002). Low content of poorly crystalline Fe oxides may retard
262 As mobilization in the solid phase, even in soils rich in Fe (Khan et al., 2010).

263 Although close linear relationships of As and Mn were also found in WS, BI, WX
264 and GZ soils except for SG soil (Fig. 2B), the role of Mn minerals may differ from Fe
265 minerals. In the 4 soils, the Mn profiles are almost identical to Fe profiles, suggesting
266 the reduction of Mn and Fe was controlled by the same group of microbial organisms
267 (Myers and Nealson, 1988). However, the correlation of As and Fe/Mn in SG soil was
268 not as well as those in other soils (Fig. 2). Furthermore, this result showed, unlike Fe
269 reduction, Mn reduction doesn't follow with As release in the top layer of SG soil
270 with low concentrations of both elements. We speculated the apparent decoupling of
271 As with Mn may be caused by two reasons, 1) Fe oxides are still abundant when Mn
272 minerals start to dissolve, which bind with the As desorbed from Mn minerals
273 (Mitsunobu et al., 2020); 2) Mn minerals catalyze the oxidation of As(III) to As(V)
274 (Chen et al., 2006), which is less mobile.



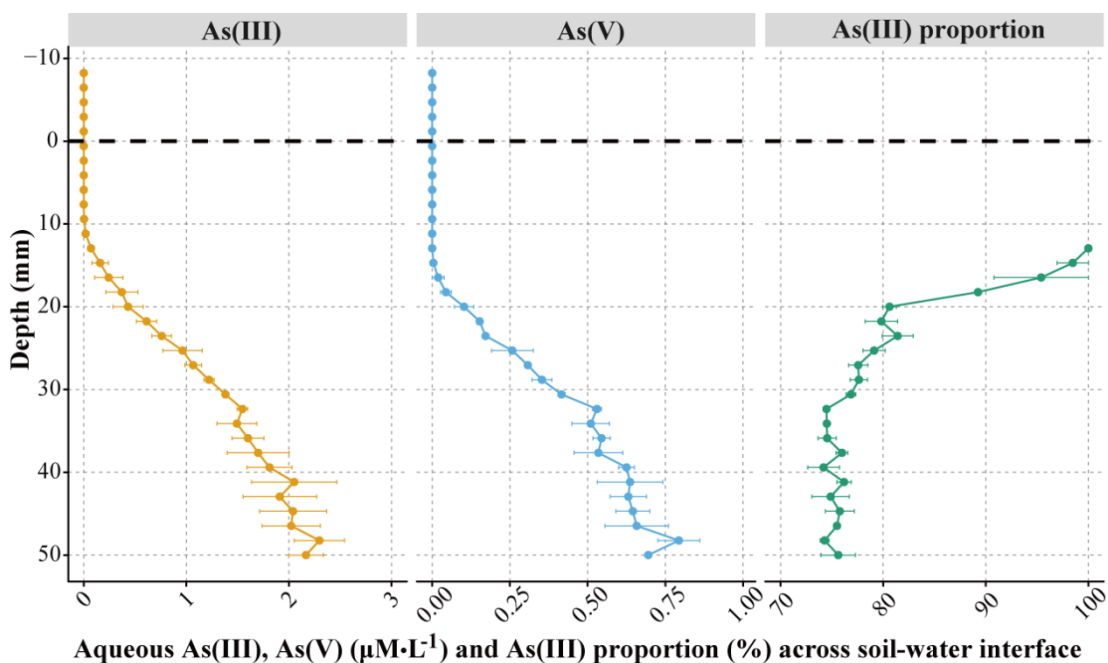
275

276 **Figure 2** The correlation between vertical aqueous As with Fe (A) and Mn (B)
 277 ($\mu\text{M}\cdot\text{L}^{-1}$) in paddy soils. Soils were collected from Wenshan (WS), Bijie (BI), Wuxue
 278 (WX), Shaoguan (SG) and Ganzhou (GZ) paddies.

279 In most cases, the cascade of Mn, As and Fe releasing to porewater along SWI is
 280 hard to spatially distinguish because their releasing zones are often overlapped
 281 (Dočekalová et al., 2002; Gao et al., 2006; Bennett et al., 2012; Arsic et al., 2018).
 282 Thus, the SG soil, which is high in Fe and Mn, is an excellent environmental sample
 283 to study the decoupling with the dominant coupling process. Regression residual
 284 analysis revealed the decoupling process happened in the oxic-anoxic transition zone

285 (Table S2). Much higher residuals were obtained in that zone of SG (residuals ≥ 0.265)
286 than in other soils with a similar regression slope (including WS, BI and WX,
287 residuals ≤ 0.0417).

288 **3.3 Speciation of As across SWI.** To reveal the arsenic speciation along Eh gradient
289 across SWI, we measured fine-scale As species profiles across the SWI of SG soil
290 (Fig. 3) and the As species at 3 depth in the other 4 soils (Table S3). Surprisingly, no
291 methyl arsenic was detected in all the samples, only As(III) and As(V) were found.
292 Although it is known that the methylation process of As is controlled by a family of
293 As(III) S-adenosylmethionine methyltransferases enzymes designated ArsM in
294 microbes or AS3MT in higher eukaryotes (Ajees and Rosen, 2015; Zhao et al., 2019),
295 the occurrence of methyl As is hard to predict in field samples. Chen et al. found that
296 the methyl As may only exist at a narrow Eh range because, when the Eh drops below
297 the Eh range, the methylotrophic methanogens capable of demethylating methyl As
298 outcompete those microbes possessing As methylating ability (Chen et al., 2019),
299 resulting in the disappearance of methyl As. According to this result, Eh only is not
300 sufficient to induce significant methyl As synthesis in the flooded soil system, as there
301 is no methylated As detected along the Eh gradient in all the soil samples. We
302 speculated that the availability of organic substrate and the functional microbial
303 community were the limiting factors in our case, more investigations are needed to
304 identify the micro-hotspot of methyl As in paddy soils.



305

306 **Figure 3** Profile of As species ($\mu\text{M}\cdot\text{L}^{-1}$) and arsenite (As(III)) proportion across the
 307 soil-water interface in Shaoguan (SG) paddy. Two As species, including As(III) and
 308 arsenate (As(V)), were detected in soil porewater.

309

In SG soil, the concentrations of As(III) and As(V) remained almost undetectable
 310 in the oxic zone but increased rapidly from 0.0070 (9.4 mm below SWI) and 0.0091
 311 (15 mm below SWI) $\mu\text{M}\cdot\text{L}^{-1}$ to as high as 2.2 and 0.75 $\mu\text{M}\cdot\text{L}^{-1}$ in reducing soils,
 312 respectively. A clear As(III) release spatially prior to As(V) is observed along SWI
 313 (Fig. 3). The similar phenomenon was only reported in marine sediments by using
 314 traditional soil slicing (Chaillou et al., 2003). Bennett et al. detected As(III) release
 315 was prior to that of ferrous Fe in the oxic-anoxic transition zone (Bennett et al., 2012).
 316 Those pieces of evidence suggested a decoupling of As(III) and Fe(II), and strong
 317 coupling of As(V) and Fe(II) in flooded soils and sediments.

318

Generally, three main processes were proposed to explain As releasing from solid
 319 Fe/Mn oxides to liquid phase. First, desorption of As from solid phase due to

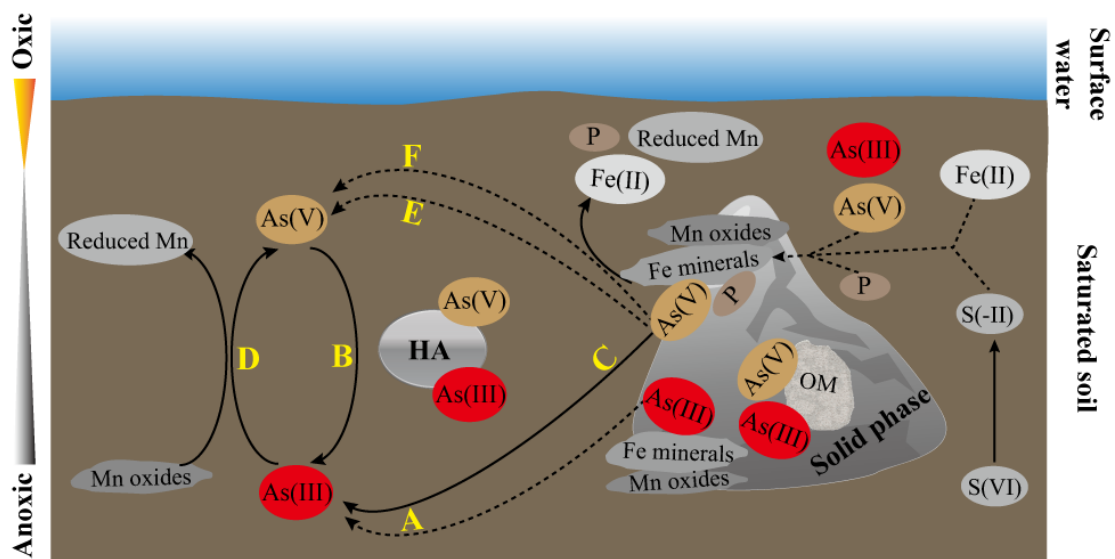
320 repartitioning of adsorbed As between solid and liquid phase (Fig. 4A&E) (Zobrist et
321 al., 2000; Williams et al., 2011). Second, the Fe(III) in the complex of Fe/Mn-As is
322 reduced to Fe(II) following As release (Fig. 4B&F) (Xu et al., 2011; Gustave et al.,
323 2018). Third, As(V) binding on Fe oxides is reduced to As(III), thus desorbed (Fig. 4C)
324 (Zhang et al., 2018). According to the redox ladder (Borch et al., 2010), the third
325 process is thermodynamically favored, which has been proven with pure minerals
326 (Tufano et al., 2008; Tufano and Scott, 2008). To the best of our knowledge, the
327 phenomenon has not been observed in saturated soils, because the latter two processes
328 were considered to occur simultaneously (Weber et al., 2010). The data presented in
329 Fig. 3 might be the first evidence from saturated soils supporting that the reduction of
330 As(V) happens on solid minerals instead of in solution.

331 Based on the As(III) and As (V) profiles, the proportion of As(III) in total As was
332 calculated and depicted in Fig. 3. The proportion change along SWI could be divided
333 into three stages: 1) a rapid decrease from 100 to 80.6% in the first 10 - 20 mm topsoil;
334 2) a slow decrease from 80.6 to 75.5% in 20 - 30 mm soils and 3) a stable value
335 (75.0 %) in deep soils (30 - 50 mm). In 30 - 50 mm below SWI (Fig. 3), the stable
336 values of As concentration (As(III) and As(V): 2.40 and 0.498 $\mu\text{M}\cdot\text{L}^{-1}$ respectively)
337 and As species in total As (75% As(III), 25% As(V)) indicate a dynamic equilibrium
338 of aqueous As(III) oxidation *vs.* As(V) reduction and their immobilization *vs.*
339 mobilization in deep soils. The immobilization process is most likely stimulated by
340 the formation of secondary sulfide S(-II) minerals (e.g. FeS) (Fig. 4), since those

341 minerals can provide additional adsorption sites for dissolved As and other elements
342 like P (Zhang and Selim, 2008; Wang et al., 2020a). The similar stable profile of As
343 was frequently reported in anoxic freshwater sediments (Bennett et al., 2012; Di et al.,
344 2012; Arsic et al., 2018). By contrast, a decrease of As along depth was captured in
345 some marine sediments rich in S (Bennett et al., 2012). Under those conditions, the
346 immobilization of As may outcompete the mobilization and lead to As decrease in
347 anoxic soils when S(VI) reduction predominates.

348 It is interesting to note that, according to the Eh-pH diagram, all the inorganic As
349 in $Eh < 0$ mV (vs. standard hydrogen electrode) should be As(III) under circumneutral
350 conditions (Akter et al., 2005). However, a considerable amount of As(V) (~ 25.0%)
351 was observed in SG soil, and the proportion was independent of soil depth in the zone
352 (Fig. 3). The persistent As(V) existence in reducing soils may represent a
353 thermodynamic equilibration of four biogeochemical processes: 1) abiotic (by Mn
354 oxides) or microbial oxidation of As(III) to As(V) (Fig. 4D) (Liu, 2006; Suda and
355 Makino, 2016; Tong et al., 2019); 2) desorption of As(V) from the solid phase due to
356 competition of adsorption sites by analogues (e.g. carbonate, bicarbonate, phosphate,
357 dissolved organic matter) (Fig. 4E) (Zobrist et al., 2000; Grafe et al., 2001; Violante
358 and Pigna, 2002; Anawar et al., 2004); 3) release of the adsorbed As(V) due to
359 microbial reduction and solubilization of the host Fe oxides (Fig. 4F) (Tufano et al.,
360 2008; Zhang et al., 2018); and 4) readily As(V) supply from humic acids (Fig. 4)
361 (Anawar et al., 2003; Chaillou et al., 2003). To verify whether there is a

362 thermodynamic equilibration of As(III) and As(V) in soil porewater, we collected the
 363 As species data from publications using typically natural soils/sediments (Table S4).
 364 The results showed dissolved As under anoxic was usually dominated by As(III), but
 365 significant As(V) (~ 20.0%) was observed in most cases (Chaillou et al., 2003; Zheng
 366 et al., 2003; Roberts et al., 2010; Somenahally et al., 2011; Hu et al., 2015; Shakoor et
 367 al., 2015; Kumar et al., 2016; Bondu et al., 2017; Xu et al., 2017; Arsic et al., 2018;
 368 Kazi et al., 2018; Lock et al., 2018; Wang et al., 2019).



369 **Figure 4** Diagram (nonspatial) depicting the processes controlling the behavior of
 370 multi-element in saturated soils. A-C) pathways contribute to As(III) enrichment in
 371 soil porewater; D-F) pathways contribute to As(V) enrichment in soil porewater. OM
 372 is solid organic matter, and HA is humic acids.
 373

374

375 4. Conclusion

376 This study investigated vertical changes of Eh, Fe, Mn, As, P, S as well as As species
 377 across SWI in paddy soils. High-resolution (mm) mapping of total aqueous Fe, Mn,

378 As, P and S by SWI profiler visibly showed one-dimensional coupling and decoupling
379 of As with Fe and Mn in different soils. Profiling of As species further identified
380 As(III) excess was the main cause of the decoupling of As with Fe and Mn in the
381 oxic-anoxic transition zone. Future studies, combining high-resolution mapping of
382 multi-element with microbial community, are essential to improve the understanding
383 of As behaviors in soils, sediments and other aquatic environments.

384

385 **Conflict of Interest**

386 The authors declare no conflict of interest.

387 **Acknowledgements**

388 This work was supported by the National Science Foundation of China (41571305,
389 41977320), Key Programme Special Fund of XJTLU (KSF-A-20). We want to thank
390 the kind help of Fuyuan Liu for designing 3D printing model. We are grateful for the
391 assistance of Yi-Li Cheng, Xiao Zhou, Xiao-Yan Zhang, and Liang-Ping Long with
392 chemical analysis.

393

394 **References**

- 395 Ajees, A.A., Rosen, B.P., 2015. As(III) S-adenosylmethionine methyltransferases and other arsenic
396 binding proteins. *Geomicrobiol. J.* 32, 570-576.
- 397 Akter, K.F., Owens, G., Davey, D.E., Naidu, R., 2005. Arsenic speciation and toxicity in biological
398 systems. *Reviews of environmental contamination and toxicology*. Springer, pp. 97-149.
- 399 Anawar, H.M., Akai, J., Komaki, K., Terao, H., Yoshioka, T., Ishizuka, T., Safiullah, S., Kato, K., 2003.
400 Geochemical occurrence of arsenic in groundwater of Bangladesh: sources and mobilization processes.
401 *J. Geochem. Explor.* 77, 109-131.
- 402 Anawar, H.M., Akai, J., Sakugawa, H., 2004. Mobilization of arsenic from subsurface sediments by
403 effect of bicarbonate ions in groundwater. *Chemosphere* 54, 753-762.
- 404 Arsic, M., Teasdale, P.R., Welsh, D.T., Johnston, S.G., Burton, E.D., Hockmann, K., Bennett, W.W.,
405 2018. Diffusive gradients in thin films (DGT) reveals antimony and arsenic mobility differs in a
406 contaminated wetland sediment during an oxic-anoxic transition. *Environ. Sci. Technol.* 52, 1118-1127.
- 407 Bennett, W.W., Teasdale, P.R., Panther, J.G., Welsh, D.T., Zhao, H., Jolley, D.F., 2012. Investigating
408 arsenic speciation and mobilization in sediments with DGT and DET: a mesocosm evaluation of
409 oxic-anoxic transitions. *Environ. Sci. Technol.* 46, 3981-3989.
- 410 Bogdan, K., Schenk, M.K., 2008. Arsenic in rice (*Oryza sativa* L.) related to dynamics of arsenic and
411 silicic acid in paddy soils. *Environ. Sci. Technol.* 42, 7885-7890.
- 412 Bondu, R., Cloutier, V., Rosa, E., Benzaazoua, M., 2017. Mobility and speciation of geogenic arsenic in
413 bedrock groundwater from the Canadian Shield in western Quebec, Canada. *Sci. Total Environ.* 574,
414 509-519.

415 Borch, T., Kretzschmar, R., Kappler, A., Cappellen, P.V., Gindervogel, M., Voegelin, A., Campbell, K.,
416 2010. Biogeochemical redox processes and their impact on contaminant dynamics. *Environ. Sci.*
417 *Technol.* 44, 15-23.

418 Bouman, B., Tuong, T.P., 2001. Field water management to save water and increase its productivity in
419 irrigated lowland rice. *Agr. Water Manage.* 49, 11-30.

420 Brannon, J., Gunnison, D., Smart, R., Chen, R., 1984. Effects of added organic matter on iron and
421 manganese redox systems in sediment. *Geomicrobiol. J.* 3, 319-341.

422 Bums, R.G., Bums, V.M., 1975. Mechanism for nucleation and growth of manganese nodules. *Nature*
423 255, 130-131.

424 Burton, E.D., Bush, R.T., Sullivan, L.A., Johnston, S.G., Hocking, R.K., 2008. Mobility of arsenic and
425 selected metals during re-flooding of iron- and organic-rich acid-sulfate soil. *Chem. Geol.* 253, 64-73.

426 Campbell, K.M., Malasam, D., Saltikov, C.W., Newman, D.K., Hering, J.G., 2006. Simultaneous
427 microbial reduction of iron (III) and arsenic (V) in suspensions of hydrous ferric oxide. *Environ. Sci.*
428 *Technol.* 40, 5950-5955.

429 Chaillou, G., Schäfer, J., Anschutz, P., Lavaux, G., Blanc, G., 2003. The behaviour of arsenic in muddy
430 sediments of the Bay of Biscay (France). *Geochim. Cosmochim. Ac.* 67, 2993-3003.

431 Chen, C., Li, L., Huang, K., Zhang, J., Xie, W.Y., Lu, Y., Dong, X., Zhao, F.J., 2019. Sulfate-reducing
432 bacteria and methanogens are involved in arsenic methylation and demethylation in paddy soils. *ISME*
433 *J.* 13, 2523-2535.

434 Chen, Z., Kim, K.W., Zhu, Y.G., McLaren, R., Liu, F., He, J.Z., 2006. Adsorption (As^{III}, V) and
435 oxidation (As^{III}) of arsenic by pedogenic Fe–Mn nodules. *Geoderma* 136, 566-572.

436 Darland, J.E., Inskeep, W.P., 1997. Effects of pH and phosphate competition on the transport of
437 arsenate. *J. Environ. Qual.* 26, 1133-1139.

438 Das, S., Liu, C.C., Jean, J.S., Lee, C.C., Yang, H.J., 2016. Effects of microbially induced
439 transformations and shift in bacterial community on arsenic mobility in arsenic-rich deep aquifer
440 sediments. *J. Hazard. Mater.* 310, 11-19.

441 Di, X., Wei, W., Shiming, D., Qin, S., Chaosheng, Z., 2012. A high-resolution dialysis technique for
442 rapid determination of dissolved reactive phosphate and ferrous iron in pore water of sediments. *Sci.*
443 *Total Environ.* 421-422, 245-252.

444 Ding, S., Wang, Y., Wang, D., Li, Y.Y., Gong, M., Zhang, C., 2016. *In situ*, high-resolution evidence for
445 iron-coupled mobilization of phosphorus in sediments. *Sci. Rep.* 6, 24341.

446 Dočekalová, H., Clarisse, O., Salomon, S., Wartel, M., 2002. Use of constrained DET probe for a
447 high-resolution determination of metals and anions distribution in the sediment pore water. *Talanta* 57,
448 145-155.

449 Frenzel, P., Rothfuss, F., Conrad, R., 1992. Oxygen profiles and methane turnover in a flooded rice
450 microcosm. *Biol. Fert. Soils* 14, 84-89.

451 Gallagher, P.A., Schwegel, C.A., Wei, X., Creed, J.T., 2001. Speciation and preservation of inorganic
452 arsenic in drinking water sources using EDTA with IC separation and ICP-MS detection. *J. Environ.*
453 *Monitor.* 3, 371-376.

454 Gao, Y., Leermakers, M., Gabelle, C., Divis, P., Billon, G., Ouddane, B., Fischer, J.C., Wartel, M.,
455 Baeyens, W., 2006. High-resolution profiles of trace metals in the pore waters of riverine sediment
456 assessed by DET and DGT. *Sci. Total Environ.* 362, 266-277.

457 Gorny, J., Billon, G., Lesven, L., Dumoulin, D., Madé, B., Noiriél, C., 2015. Arsenic behavior in river
458 sediments under redox gradient: a review. *Sci. Total Environ.* 505, 423-434.

459 Grafe, M., Eick, M., Grossl, P., 2001. Adsorption of arsenate (V) and arsenite (III) on goethite in the
460 presence and absence of dissolved organic carbon. *Soil Sci. Soc. Am. J.* 65, 1680-1687.

461 Gustave, W., Yuan, Z.F., Ren, Y.X., Sekar, R., Chen, Z., 2019a. Arsenic alleviation in rice by using
462 paddy soil microbial fuel cells. *Plant Soil* 441, 111-127.

463 Gustave, W., Yuan, Z.F., Sekar, R., Ren, Y.X., Chang, H.C., Liu, J.Y., Chen, Z., 2018. The change in
464 biotic and abiotic soil components influenced by paddy soil microbial fuel cells loaded with various
465 resistances. *J. Soil. Sediment.* 19, 106-115.

466 Gustave, W., Yuan, Z.F., Sekar, R., Ren, Y.X., Liu, J.Y., Zhang, J., Chen, Z., 2019b. Soil organic matter
467 amount determines the behavior of iron and arsenic in paddy soil with microbial fuel cells.
468 *Chemosphere* 237, 124459.

469 Honma, T., Ohba, H., Kaneko-Kadokura, A., Makino, T., Nakamura, K., Katou, H., 2016. Optimal soil
470 Eh, pH, and water management for simultaneously minimizing arsenic and cadmium concentrations in
471 rice grains. *Environ. Sci. Technol.* 50, 4178-4185.

472 Hu, P., Ouyang, Y., Wu, L., Shen, L., Luo, Y., Christie, P., 2015. Effects of water management on
473 arsenic and cadmium speciation and accumulation in an upland rice cultivar. *J. Environ. Sci.* 27,
474 225-231.

475 Islam, F.S., Gault, A.G., Boothman, C., Polya, D.A., Chamock, J.M., Chatterjee, D., Lloyd, J.R., 2004.
476 Role of metal-reducing bacteria in arsenic release from Bengal delta sediments. *Nature* 430, 68-71.

477 Kazi, T.G., Brahman, K.D., Baig, J.A., Afridi, H.I., 2018. A new efficient indigenous material for

478 simultaneous removal of fluoride and inorganic arsenic species from groundwater. *J. Hazard. Mater.*
479 357, 159-167.

480 Khan, M.A., Stroud, J.L., Zhu, Y.G., McGrath, S.P., Zhao, F.J., 2010. Arsenic bioavailability to rice is
481 elevated in Bangladeshi paddy soils. *Environ. Sci. Technol.* 44, 8515-8521.

482 Kumar, M., Ramanathan, A., Rahman, M.M., Naidu, R., 2016. Concentrations of inorganic arsenic in
483 groundwater, agricultural soils and subsurface sediments from the middle Gangetic plain of Bihar,
484 India. *Sci. Total Environ.* 573, 1103-1114.

485 Liu, F., 2006. Arsenite oxidation by three types of manganese oxides. *J. Environ. Sci.* 18, 292-298.

486 Lock, A., Wallschläger, D., Belzile, N., Spiers, G., Gueguen, C., 2018. Rates and processes affecting As
487 speciation and mobility in lake sediments during aging. *J. Environ. Sci.* 66, 338-347.

488 Ma, W.W., Zhu, M.X., Yang, G.P., Li, T., 2017. In situ, high-resolution DGT measurements of
489 dissolved sulfide, iron and phosphorus in sediments of the East China Sea: Insights into phosphorus
490 mobilization and microbial iron reduction. *Mar. Pollut. Bull.* 124, 400-410.

491 Masscheleyn, P.H., Delaune, R.D., Patrick Jr, W.H., 1991. Effect of redox potential and pH on arsenic
492 speciation and solubility in a contaminated soil. *Environ. Sci. Technol.* 25, 1414-1419.

493 Meharg, A.A., 2004. Arsenic in rice—understanding a new disaster for South-East Asia. *Trends Plant*
494 *Sci.* 9, 415-417.

495 Mitsunobu, S., Toda, M., Hamamura, N., Shiraishi, F., Tominaga, Y., Sakata, M., 2020.
496 Millimeter-scale topsoil layer blocks arsenic migration in flooded paddy soil. *Geochim. Cosmochim.*
497 *Ac.* 274, 211-227.

498 Mucci, A., Richard, L.F., Lucotte, M., Guignard, C., 2000. The differential geochemical behavior of

499 arsenic and phosphorus in the water column and sediments of the Saguenay Fjord estuary, Canada.
500 *Aquat. Geochem.* 6, 293-324.

501 Myers, C.R., Nealson, K.H., 1988. Microbial reduction of manganese oxides: Interactions with iron
502 and sulfur. *Geochim. Cosmochim. Ac.* 52, 2727-2732.

503 Pester, M., Knorr, K.H., Friedrich, M.W., Wagner, M., Loy, A., 2012. Sulfate-reducing microorganisms
504 in wetlands—fameless actors in carbon cycling and climate change. *Front. Microbiol.* 3, 72.

505 Polizzotto, M.L., Kocar, B.D., Benner, S.G., Sampson, M., Fendorf, S., 2008. Near-surface wetland
506 sediments as a source of arsenic release to ground water in Asia. *Nature* 454, 505-508.

507 Roberts, L.C., Hug, S.J., Voegelin, A., Dittmar, J., Kretzschmar, R., Wehrli, B., Saha, G.C.,
508 Badruzzaman, A.B.M., Ali, M.A., 2010. Arsenic dynamics in porewater of an intermittently irrigated
509 paddy field in Bangladesh. *Environ. Sci. Technol.* 45, 971-976.

510 Shakoor, M., Niazi, N., Bibi, I., Rahman, M., Naidu, R., Dong, Z., Shahid, M., Arshad, M., 2015.
511 Unraveling health risk and speciation of arsenic from groundwater in rural areas of Punjab, Pakistan.
512 *Int. J. Environ. Res. Pub. He.* 12, 12371-12390.

513 Somenahally, A.C., Hollister, E.B., Yan, W., Gentry, T.J., Loeppert, R.H., 2011. Water management
514 impacts on arsenic speciation and iron-reducing bacteria in contrasting rice-rhizosphere compartments.
515 *Environ. Sci. Technol.* 45, 8328-8335.

516 Suda, A., Makino, T., 2016. Functional effects of manganese and iron oxides on the dynamics of trace
517 elements in soils with a special focus on arsenic and cadmium: a review. *Geoderma* 270, 68-75.

518 Suzuki, Y., Shimoda, Y., Endo, Y., Hata, A., Yamanaka, K., Endo, G., 2009. Rapid and effective
519 speciation analysis of arsenic compounds in human urine using anion-exchange columns in

520 HPLC-ICP-MS. *J. Occup. Health* 51, 380-385.

521 Takahashi, Y., Minamikawa, R., Hattori, K.H., Kurishima, K., Kihou, N., Yuita, K., 2004. Arsenic
522 behavior in paddy fields during the cycle of flooded and non-flooded periods. *Environ. Sci. Technol.* 38,
523 1038-1044.

524 Tong, H., Liu, C., Hao, L., Swanner, E.D., Chen, M., Li, F., Xia, Y., Liu, Y., Liu, Y., 2019. Biological
525 Fe(II) and As(III) oxidation immobilizes arsenic in micro-oxic environments. *Geochim. Cosmochim.*
526 *Ac.* 265, 96-108.

527 Tufano, K.J., Reyes, C., Saltikov, C.W., Fendorf, S., 2008. Reductive processes controlling arsenic
528 retention: revealing the relative importance of iron and arsenic reduction. *Environ. Sci. Technol.* 42,
529 8283-8289.

530 Tufano, K.J., Scott, F., 2008. Confounding impacts of iron reduction on arsenic retention. *Environ. Sci.*
531 *Technol.* 42, 4777-4783.

532 Violante, A., Pigna, M., 2002. Competitive sorption of arsenate and phosphate on different clay
533 minerals and soils. *Soil Sci. Soc. Am. J.* 66, 1788-1796.

534 Wang, H.Y., Byrne, J.M., Perez, J.P.H., Thomas, A.N., Göttlicher, J., Höfer, H.E., Mayanna, S., Kontny,
535 A., Kappler, A., Guo, H.M., Benning, L.G., Norra, S., 2020a. Arsenic sequestration in pyrite and
536 greigite in the buried peat of As-contaminated aquifers. *Geochim. Cosmochim. Ac.* 284, 107-119.

537 Wang, J., Kerl, C.F., Hu, P., Martin, M., Mu, T., Brüggewirth, L., Wu, G., Said-Pullicino, D., Romani,
538 M., Wu, L., 2020b. Thiolated arsenic species observed in rice paddy pore waters. *Nature Geosci.* 13,
539 282-287.

540 Wang, M., Tang, Z., Chen, X.P., Wang, X., Zhou, W.X., Tang, Z., Zhang, J., Zhao, F.J., 2019. Water

541 management impacts the soil microbial communities and total arsenic and methylated arsenicals in rice
542 grains. *Environ. Pollut.* 247, 736-744.

543 Weber, F.A., Hofacker, A.F., Voegelin, A., Kretzschmar, R., 2010. Temperature dependence and
544 coupling of iron and arsenic reduction and release during flooding of a contaminated soil. *Environ. Sci.*
545 *Technol.* 44, 116-122.

546 White, B.P., Mulligan, S., Merrill, K., Wright, J., 2007. An examination of the relationships between
547 motor and process skills and scores on the sensory profile. *Appl. Environ. Microb.* 61, 154-160.

548 Widerlund, A., Davison, W., 2007. Size and density distribution of sulfide-producing microniches in
549 lake sediments. *Environ. Sci. Technol.* 41, 8044-8049.

550 Williams, P.N., Zhang, H., Davison, W., Meharg, A.A., Hossain, M., Norton, G.J., Brammer, H., Islam,
551 M.R., 2011. Organic matter-solid phase interactions are critical for predicting arsenic release and plant
552 uptake in Bangladesh paddy soils. *Environ. Sci. Technol.* 45, 6080-6087.

553 Wu, Z., Jiao, L., Wang, S., Xu, Y., 2016a. Multi-metals measured at sediment-water interface (SWI) by
554 diffusive gradients in thin films (DGT) technique for geochemical research. *Arch. Environ. Con. Tox.*
555 70, 429-437.

556 Wu, Z., Ren, D., Zhou, H., Hang, G., Li, J., 2016b. Sulfate reduction and formation of iron sulfide
557 minerals in nearshore sediments from Qi'ao Island, Pearl River Estuary, Southern China. *Quatern. Int.*
558 452, 137-147.

559 Xiu, W., Guo, H., Shen, J., Liu, S., Ding, S., Hou, W., Ma, J., Dong, H., 2016. Stimulation of Fe (II)
560 oxidation, biogenic lepidocrocite formation, and arsenic immobilization by *Pseudogulbenkiania* sp.
561 strain 2002. *Environ. Sci. Technol.* 50, 6449-6458.

562 Xu, W., Wang, H., Liu, R., Zhao, X., Qu, J., 2011. Arsenic release from arsenic-bearing Fe–Mn binary
563 oxide: Effects of Eh condition. *Chemosphere* 83, 1020-1027.

564 Xu, X., Chen, C., Wang, P., Kretzschmar, R., Zhao, F.J., 2017. Control of arsenic mobilization in paddy
565 soils by manganese and iron oxides. *Environ. Pollut.* 231, 37-47.

566 Yuan, Z.-F., Gustave, W., Sekar, R., Bridge, J., Wang, J.-Y., Feng, W.-J., Guo, B., Chen, Z., 2021.
567 Simultaneous measurement of aqueous redox-sensitive elements and their species across the soil-water
568 interface. *J. Environ. Sci.* 102, 1-10.

569 Yuan, Z.F., Ata-Ul-Karim, S.T., Cao, Q., Lu, Z., Cao, W., Zhu, Y., Liu, X., 2016. Indicators for
570 diagnosing nitrogen status of rice based on chlorophyll meter readings. *Field Crops Res.* 185, 12-20.

571 Yuan, Z.F., Gustave, W., Bridge, J., Liang, Y., Sekar, R., Boyle, J., Jin, C.Y., Pu, T.Y., Ren, Y.X., Chen,
572 Z., 2019. Tracing the dynamic changes of element profiles by novel soil porewater samplers with
573 ultralow disturbance to soil–water interface. *Environ. Sci. Technol.* 53, 5124-5132.

574 Zachara, J.M., Kukkadapu, R.K., Fredrickson, J.K., Gorby, Y.A., Smith, S.C., 2002. Biomineralization
575 of poorly crystalline Fe(III) oxides by dissimilatory metal reducing bacteria (DMRB). *Geomicrobiol. J.*
576 19, 179-207.

577 Zhang, H., Selim, H.M., 2008. Competitive sorption-desorption kinetics of arsenate and phosphate in
578 soils. *Soil Sci.* 173, 3-12.

579 Zhang, J., Ma, T., Yan, Y., Xie, X., Abass, O.K., Liu, C., Zhao, Z., Wang, Z., 2018. Effects of Fe-S-As
580 coupled redox processes on arsenic mobilization in shallow aquifers of Datong Basin, northern China.
581 *Environ. Pollut.* 237, 28-38.

582 Zhao, Y., Su, J., Ye, J., Rensing, C., Tardif, S., Zhu, Y., Brandt, K.K., 2019. AsChip: a high-throughput

583 qPCR chip for comprehensive profiling of genes linked to microbial cycling of arsenic. *Environ. Sci.*
584 *Technol.* 53, 798-807.

585 Zheng, J., Hintelmann, H., Dimock, B., Dzurko, M.S., 2003. Speciation of arsenic in water, sediment,
586 and plants of the Moira watershed, Canada, using HPLC coupled to high resolution ICP-MS. *Anal.*
587 *Bioanal. Chem.* 377, 14-24.

588 Zobrist, J., Dowdle, P.R., Davis, J.A., Oremland, R.S., 2000. Mobilization of arsenite by dissimilatory
589 reduction of adsorbed arsenate. *Environ. Sci. Technol.* 34, 4747-4753.